CHARACTERIZATION OF THE VSCOELASTIC PROPERTIES WITH MAGENTIC RESONANCE ELASTOGRAPHY (MRE) TECHNIQUE: APPLICATIONS TO PHANTOMS AND LIVERS TISSUES

S. Bensamoun, M. Chakouch
UTC - Laboratoire de Biomécanique et Bioingénierie, UMR CNRS 7338, Rue Roger Couttolenc, CS 60319, 60203 Compiègne Téléphone : 03 44 23 43 90,
Adresses électroniques: sabine.bensamoun@utc.fr, mashhour.chakouch@utc.fr

Key words: Phantom, Liver, mechanical properties, elastography, MRI

1. INTRODUCTION

Magnetic resonance elastography (MRE) technique was applied to different healthy (Chakouch et al. 2015) and pathological soft tissues (Venkatesh et al. 2008, Bensamoun et al. 2015), in order to provide quantitative stiffness data to the clinician from superficial to deep areas. Currently, this noninvasive MRE method is only used in clinical practice for liver test, allowing the assessment of the fibrosis level (Yin et al. 2015). This diagnosis was based on the stiffness (shear modulus) measurement revealing higher values for pathological tissues (Bensamoun et al. 2013).

Subsequently, MRE technique was extensively improved for the characterization of the viscoelastic behavior, revealing the fluid and solid components of the soft tissues (Klatt et al. 2007). Thus, the viscoelastic properties of the liver (Leclerc et al. 2013), brain (Klatt et al. 2007) and muscle (Debernard et al 2013) were determined with multi-frequency MRE tests. These measurements were obtained with the development of imaging sequences and reconstruction methods (Hirsch et al. 2014) in order to acquire the cartographies of the storage modulus (G') and the loss modulus (G'') which compose the viscoelastic properties.

All of these developments were mainly tested on phantoms composed of different materials (wirosil (Kolipaka et al. 2009), agarose (Chen et al. 2005), bovine gel (Yin et al. 2008) mimicking the elastic properties of soft tissues (Chakouch et al. 2014) and dynamic organs (Kolipaka et al. 2010). Indeed, at first organic gels (agarose, bovine) were used for their accessibilities but the main inconvenience was the stability of the material as a function of time. Subsequently, wirosil phantoms were used due to their stability compared to the organic gels. However, this material showed high stiffness which was not adapted for liver tissue. Some phantoms (CIRS Inc) were commercially available for ultrasound elastography (Amador et al. 2012), but the inconvenience was the fixed Young's modulus, determined only at low frequencies, provided by the constructor. In the literature many studies created their own phantoms composed of polymer (PVC) (Chakouch et al. 2015) in ordre to control and perform different ranges of stiffness corresponding to biological tissues and to produce stable elastic properties as a function of time (Leclerc et al. 2012). Recently, Nguyen's team has developed oil-in-gelatin phantoms to measure the shear modulus and the viscosity (Nguyen et al. 2013).

The phantoms are considered as a benchmark for medical imaging techniques. Thus, the purpose of this study was to develop phantoms mimicking the viscoelastic properties of different healthy and fibrotic livers using MRE technique.

2. MATERIALS AND METHODS

2.1 Phantom preparation

Homogeneous phantoms were created with different concentrations of liquid plastic (Plastileurre, Bricoleurre, France) and softener (Assouplissant, Bricoleurre, France) in order to mimic the different stages of the liver fibrosis. The liquid plastic, also called plastisol, is a suspension of PVC particles in a solvent. The mixture was adjusted from 40% to 60% with a step concentration of 10%, in order to progressively increase the stiffness of the media, and heated to 177°C. Subsequently, the solution was poured into aluminum molds, which were resistant to high temperature, in order to create three homogeneous parallelepiped (length: 14 cm, width: 7 cm, and height: 5 cm, Fig. 1) phantoms used for MRE technique. The different molds were left to cool to room temperature (23°C) until the phantoms solidified. The density of the phantoms was experimentally evaluated (1000 ± 47 kg/m^3). Then, the phantoms were preserved and stocked at room temperature (23°C).

2.2 Phantom Magnetic Resonance Elastography (MRE) tests

The phantom was placed inside a head coil in a 1.5T MRI machine (Signa HDx, GE) (Fig. 1). A cylindrical driver, currently used in clinical practice for liver MRE test, was positioned below the phantom. Moreover, a soft MRI cushion was inserted between the phantom and the driver in order to avoid motion artifacts during the test. The driver is connected via a long tube to a loudspeaker, located in the MRI technical room, which generates air pressure at low frequency 60 Hz. The phase images, showing the displacement of the shear waves inside the parallelepiped phantoms, were collected with: four offsets, a gradient echo sequence, an acquisition matrix of 256 x 64 (interpolated to 256 x 256), a flip angle of 45°, a field of view of 20 cm, TR equal to 50 ms and TE corresponding to the minimum echo time allowing for motion encoding.

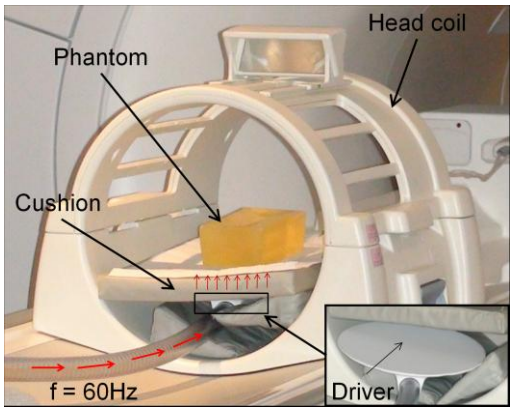

Figure 1. Set up of the magnetic resonance elastography tests performed on the different phantoms

2.3 Liver Magnetic Resonance Elastography (MRE) tests

Healthy participants (N = 10), with no history of liver disease, were recruited and two groups of patients characterized with minor (N = 20) and major (N = 10) fibrosis were recruited from the alcoholism department. The stage of fibrosis was determined with the Fibroscan (EchoSens) exam due to the risk induced by the biopsy which is an unnecessary procedure for alcoholic patients. The classification of the level of fibrosis was based on the METAVIR Score (Bedossa et al. 1994) with F0: healthy liver, F1-F2: minor fibrosis and F3-F4: major fibrosis.
Subject were placed in a supine position in a 1.5T MRI machine (Signa HDx, GE), and the cylindrical liver acoustic driver, used for the previous phantom MRE tests (Fig. 1), was positioned in contact with the ribcage at the same level as the diaphragm. Similarly to the phantom, shear waves were propagated within the liver at a single frequency of 60 Hz. Phase images (4 offsets) were recorded with a motion sensitizing gradient echo sequence, a flip angle of 30°, a field of view between 36 and 48 cm, a 256 x 64 acquisition matrix, a TE = 26.8 ms and a TR = 100 msec. The total scan time was 32 seconds, corresponding to two breath-holding periods of 16 seconds.

2.4 MRE Post-processing

The recorded phase images underwent post-processing by applying a mask, which removed the noise located in the background of the image. The viscoelastic properties of the phantoms and liver tissues were obtained with the two following methods. The first one provides a local stiffness measurement by prescribing a 1D profile drawn along the direction of the shear wave propagation (Fig.2, 3).
Assuming that the media (phantom or liver tissue) was linearly elastic, isotropic, incompressible and homogeneous, the local shear stiffness (μ) representing the local elasticity was calculated using the following equation $\mu = \rho.(f.\lambda)^2$, where ρ is the density assumed to be closed to the water (1000 kg/m^3). The wavelength (□ was determined by considering the distance between consecutive picks. The second method applied an inversion algorithm to the phase images to represent the viscoelastic properties (Manduca et al. 2001) through the cartographies of the storage (G') and the loss (G'') modulus. Regions of interests (ROI) were placed on cartographies to measure the average data with the standard deviation.

3 RESULTS

3.1 Viscoelastic properties of the phantoms as a function of the plastic concentration

The results of the MRE tests performed on the phantoms are summarized in Fig. 2. The phase images revealed a clear propagation of the shear waves within the different phantoms with an increase of the wavelength as a function of the plastic concentration. The results of the local (μ) and global (G') elastic values were in the same range and increase with the level of the plastic concentration.

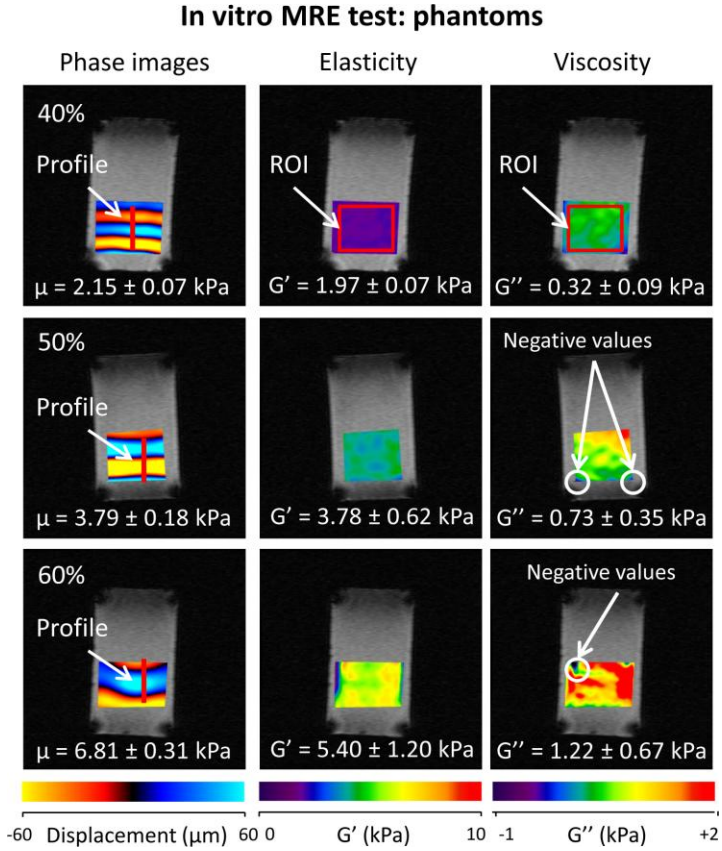

Figure 2. Phase images (60 Hz) with a red profile providing the local stiffness for the different phantoms. Cartographies of G' and G'', obtained with inversion algorithm, provide a global stiffness measured inside the represented ROI

The range of viscous data was smaller (from 0.24 kPa to 1.22 kPa) compared to the range of the G' values (from 0.89 kPa to 5.40 kPa). The viscous properties increase also as a function of the plastic concentration (Fig. 2).

3.2 Viscoelastic properties of the healthy and fibrotic livers

Phase images showed a clear propagation of the shear waves within the healthy and fibrotic livers, and as expected the wavelength increased with the level of fibrosis (Fig. 3). The average storage modulus (G') for healthy, minor and major fibrosis were 1.82 ± 0.23 kPa, 3.78 ± 0.74 kPa and 5.52 ± 1.03 kPa, respectively. The loss modulus (G'') was in the same range for healthy (0.51 ± 0.17 kPa) and minor (0.56 ± 0.25 kPa) fibrosis while a slight increase was measured for the major (0.84 ± 0.44 kPa) fibrosis.

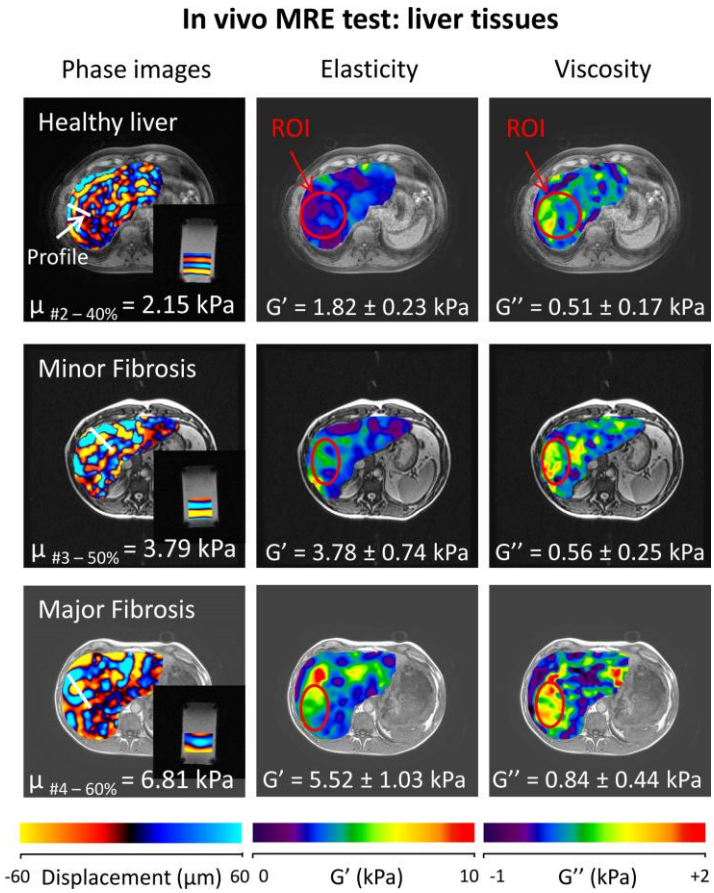

Figure 3. Phase images and cartographies (G' and G'') obtained for healthy and fibrotic liver.

3.3 Analogy between the MRE viscoelastic properties of the phantoms and different biological tissues (livers, …)

MRE technique was also applied, by the same team, with the same set up (60 Hz, liver driver) to other tissues (spleen, kidney and muscle).

The result of the elastic properties of the phantom 40% (G'_40% = 1.97 ± 0.07 kPa) mimics the elastic behavior of the F0 liver (G'_F0 = 1.82 ± 0.23 kPa). Furthermore, the elastic behaviors of the psoas (2.60 ± 0.25 kPa) (Bensamoun et al. 2011) and vastus medialis (2.64 ± 0.20 kPa) (Debernard

et al. 2013) in passive (i.e. at rest) condition were also in the same range as the phantoms made with 40 % of plastic.
The phantom with 50 % of plastic revealed elastic property (G'_50% = 3.78 ± 0.62 kPa) close to minor (F1, F2) fibrosis stages (G'_minor = 3.78 ± 0.74 kPa). This phantom could be used to mimic the elastic properties of these liver stages. In comparison to other tissues such as the kidney (4.37 ± 0.59 kPa) (Bensamoun et al. 2011), the spleen (4.75 ± 0.70 kPa) and the sartorius muscle (4.13 ± 0.69 kPa (Debernard et al. 2013)) at rest, the phantom 50% could be used to represent the elastic properties of these tissues.
The last phantom (60 %) had elastic properties (G'_60% = 5.40 ± 1.20 kPa) corresponding to the ones of the major liver fibrosis (i.e. stage F3-F4) (G'_major = 5.52 ± 1.03 kPa). In comparison to muscle studies, this phantom could be used to mimic the elastic properties of the semitendinosus (ST) muscle at rest ($\mu_{\_ ST}$ = 5.32 ± 0.10 kPa) (Chakouch et al. 2015).
Concerning the viscous properties, only the 50 % phantom revealed data (G"_50% = 0.73 ± 0.35 kPa) close to the major fibrosis (G" _major = 0.84 ± 0.44 kPa).

4. DISCUSSION

Magnetic resonance elastography (MRE) is now a clinical liver test to diagnose the extent of liver fibrosis. The further development of MRE methods has revealed utility for other medical applications (brain, breast). It is well known that the phantoms have always been considered as a necessary object for the calibration of imaging sequences used by CT scanners, MRI machines or ultrasound (US). To our knowledge, any phantom dedicated to MRE technique was developed by imaging companies while ultrasound elastography employs specific commercial phantoms for the characterization of breast and liver tissues. These tests objects are certified by the company as compatible with MRI machines, and it was therefore expected to get MRE phase images by applying MRE sequence. However, the recent liver phantom (Model 057, CIRS, Norfolk, Virginia, USA), used for US elastography, was not MRE compatible and it was impossible to record phase images using the MRE liver sequence. As a consequence, there is a real clinical need for a MRE benchmark before performing in vivo MRE tests. The originality of the present study was to develop plastic phantoms allowing for the simulation of the viscoelastic properties of liver tissues enabling clinicians to choose the appropriate phantom as a function of the fibrosis levels.

In addition to the simulation of the functional (elasticity, viscosity, density) behavior of the biological tissue, the development of a phantom also required to take into account the characteristics (driver, frequency, MR sequence) of the MRE protocol used in clinic. Indeed, the material properties (pneumatic, mechanical) and the shape (round, tube) of the driver were key points to ensure the generation of the shear wave within the tissue (Chakouch et al. 2015). Thus, in the present study the same driver as the one applied for liver MRE tests in clinical practice was used in order to attenuate the eventual effects of the driver on the shear wave propagation. Furthermore, the frequency applied during the MRE test is also an important parameter of the protocol due to the frequency-dependence, or viscoelastic properties of the soft tissues. In the literature, the current range of frequency performed on human tissues, with MRE technique, is between 25 Hz and 110 Hz (Klatt et al. 2007), (Debernard et al. 2013). Therefore, the developed phantoms should work for this biological range of frequencies. Phantoms made of wirosil were extensively used by other studies (Kolipaka et al. 2009), to obtain a clear propagation of the shear wave within the material, but the mechanical behaviors (144 kPa) were not comparable to biological soft tissues. Indeed, the use of wirosil phantoms required higher MRE frequencies (200 Hz) (Kolipaka et al. 2009) compared to soft tissues (for instance: 60 Hz for the liver, 90 Hz for the muscle). Subsequently, plastisol material was used, enabling one to vary the plastic liquid concentration, in order to better mimic the elastic properties of biological tissues and to use similar frequency MRE ranges as in vivo studies. Thus, Baghani et al. (2009) have shown an increase of shear stiffness with the level of concentration using ultrasound elastography (Baghani et al. 2009).

The development of the present phantoms revealed some shape limitations related to the chosen dimension. Indeed, the height was not appropriate for the large wavelength obtained for high plastic concentration. Therefore, it was difficult to visualize at least one wavelength for the stiffer phantom (60 %), and higher molds must be used for future MRE tests. Moreover, the inversion algorithm used in this present study should be improved due to the presence of negative viscous values. These data were found in the boundary areas of the loss modulus cartography due to the reflected waves and the presence of noise. This phenomenon was emphasized for a stiffer media. Thus, these zones were carefully avoiding during the selection of the region of interest (ROI).

This preliminary set of phantoms revealed the possibility to mimic the elastic (storage modulus) properties of healthy and pathological livers. In perspective, the phantom must be further developed to better characterize the viscous properties of the livers. In addition, the composition of the phantoms may be enhanced to have a more real phantom to mimic the anisotropic and inhomogeneous behavior of the brain, skeletal muscle, kidney, etc ...

REFERENCES

Gens A., Alonso E. E. et Hight D. W., "Special problem soils: general review", *Int. J. of Something*, **35**, 2, (2004), pp. 152-859.

Wu Y. & Zhong X., "The mathematics of telephone numbers", *Annals of Improbable Research*, **1**, 5, (1995), pp. 162-163.

Amador C., Urban M. W., Chen S., et Greenleaf J. F., "Loss tangent and complex modulus estimated by acoustic radiation force creep and shear wave dispersion" , *Phys. Med. Biol.*, 57, 5, (2012), pp. 1263–1282.

Baghani A., Eskandari H., Salcudean S., et Rohling R., "Measurement of viscoelastic properties of tissue-mimicking material using longitudinal wave excitation" , *Ultrason. Ferroelectr. Freq. Control IEEE Trans. On*, 56, 7, (2009), pp. 1405 –1418.

Bedossa P., "Intraobserver and Interobserver Variations in Liver Biopsy Interpretation in Patients with Chronic Hepatitis C" , *Hepatology*, 20, 1, (1994), pp. 15–20.

Bensamoun S. F., Robert L., Leclerc G. E., Debernard L., et F. Charleux, "Stiffness imaging of the kidney and adjacent abdominal tissues measured simultaneously using magnetic resonance elastography" , *Clin. Imaging*, 35, 4, (2011), pp. 284–287.

Bensamoun S. F., Charleux F., et Themar-Noel C., "Elastic properties of skeletal muscle and subcutaneous tissues in Duchenne muscular dystrophy by magnetic resonance elastography (MRE): a feasibility study" , *Innovation and Research in BioMedical engineering (IRBM).*, 2015.

Bensamoun S. F., Leclerc G. E., Debernard L., Cheng X., Robert L., Charleux F., Rhein C., et J. P. Latrive, "Cutoff Values for Alcoholic Liver Fibrosis Using Magnetic Resonance Elastography Technique" , *Alcohol. Clin. Exp. Res.*, 37, 5, (2013), pp. 811–817.

Chakouch M. K., Charleux F., et Bensamoun S. F., "New magnetic resonance elastography protocols to characterise deep back and thigh muscles" , *Comput. Methods Biomech. Biomed. Engin.*, 17 Suppl 1, (2014), pp. 32–33.

Chakouch M. K., Charleux F., et Bensamoun S. F., “Definition of imaging plans for quantifying elastic property of nine thigh muscles using magnetic resonance elastography (MRE)” , *PLoS ONE*, (2015), In press.

Chakouch M. K., Charleux F., et Bensamoun S. F., “Development of a phantom mimicking the functional and structural behaviors of the thigh muscles characterized with magnetic resonance elastography technique” , *IEEE Engineering in Medicine and Biology Society*, (2015).

Chen Q., Ringleb S. I., Hulshizer T., et An K. N., “Identification of the testing parameters in high frequency dynamic shear measurement on agarose gels” , *J. Biomech.*, 38, 4, (2005), pp. 959–963.

Debernard L., Leclerc G. E., Robert L., Charleux F., et Bensamoun S. F., “*In vivo* Characterization of the muscle viscoelasticity in passive and active conditions using multifrequency MR Elastography” , *J. Musculoskelet. Res.*, 16, 2, (2013), pp. 1350008.

Hirsch S., Guo J., Reiter R., Papazoglou S., Kroencke T., Braun J., et Sack I., “MR Elastography of the Liver and the Spleen Using a Piezoelectric Driver, Single-Shot Wave-Field Acquisition, and Multifrequency Dual Parameter Reconstruction” , *Magn. Reson. Med.*, 71, 1, (2014), pp. 267–277.

Klatt D., Hamhaber U., Asbach P., Braun J., et Sack I., “Noninvasive assessment of the rheological behavior of human organs using multifrequency MR elastography: a study of brain and liver viscoelasticity” , *Phys. Med. Biol.*, 52, 24, (2007), pp. 7281–7294.

Kolipaka A., McGee K. P., Araoz P. A., Glaser K. J., Manduca A., et Ehman R. L., “Evaluation of a rapid, multiphase MRE sequence in a heart-simulating phantom” , *Magn. Reson. Med.*, 62, 3, (2009), pp. 691–698.

Leclerc G. E., Charleux F., Robert L., Ho Ba Tho M. C., Rhein C., Latrive J. P., et Bensamoun S. F., “Analysis of liver viscosity behavior as a function of multifrequency magnetic resonance elastography (MMRE) postprocessing” , *J. Magn. Reson. Imaging*, 38, 2, (2013), pp. 422–428.

Leclerc G. E., Debernard L., Foucart F., Robert L., Pelletier K. M., Charleux F., Ehman R., Ho Ba Tho M.-C., et Bensamoun S. F., “Characterization of a hyper-viscoelastic phantom mimicking biological soft tissue using an abdominal pneumatic driver with magnetic resonance elastography (MRE)” , *J. Biomech.*, 45, 6, (2012), pp. 952–957.

Manduca A., Oliphant T. E., Dresner M. A., Mahowald J. L., Kruse S. A., Amromin E., Felmlee J. P., Greenleaf J. F., et Ehman R. L., “Magnetic resonance elastography: Non-invasive mapping of tissue elasticity” , *Med. Image Anal.*, 5, 4, (2001), pp. 237–254.

Nguyen M. M., Zhou S., Robert J., Shamdasani V., et Xie H., “Development of Oil-in-Gelatin Phantoms for Viscoelasticity Measurement in Ultrasound Shear Wave Elastography” , *Ultrasound Med. Biol.*, 40, 1, (2014), pp. 168-176.

Venkatesh S. K., Yin M., Glockner J. F., Takahashi N., Araoz P. A., Talwalkar J. A., et Ehman R. L., “Magnetic Resonance Elastography of Liver Tumors- Preliminary Results,” *AJR Am. J. Roentgenol.*, 190, 6, (2008), pp. 1534–1540.

Yin M., Glaser K. J., Talwalkar J. A., Chen J., Manduca A., et R. L. Ehman, “Hepatic MR Elastography: Clinical Performance in a Series of 1377 Consecutive Examinations” , *Radiology*, 8, (2015), pp.142141.

Yin M., Rouvière O., Glaser K. J., et Ehman R. L., “Diffraction-biased shear wave fields generated with longitudinal magnetic resonance elastography drivers” , *Magn. Reson. Imaging*, 26, 6, (2008), pp. 770–780.